Pakistan Veterinary Journal

ISSN: 0253-8318 (PRINT), 2074-7764 (ONLINE)
DOI: 10.29261/pakvetj/2024.237

RESEARCH ARTICLE

Evaluation of Pancreatic Exocrine Function by Secretin-Enhanced Magnetic Resonance Cholangiopancreatography in Dogs Associated Acute Edematous Pancreatitis

Yue Yuan1, De Ji Yang1, Chu Qiao He1, Zong Tao Shu1, Xiao Kun Li2, Da Wei Yao1*

[1]Diagnostic Imaging Center of Veterinary Medicine, College of Veterinary Medicine, Nanjing Agricultural University, Nanjing, China; [2]Zhongnong Jinxiu Animal Hospital, Beijing, China.
*Corresponding author: yaodawei@njau.edu.cn

ARTICLE HISTORY (24-291)

Received: May 26, 2024
Revised: August 15, 2024
Accepted: August 17, 2024
Published online: August 27, 2024

Key words:
Dogs
Acute edematous pancreatitis
MRCP
Secretin
Pancreatic exocrine function

ABSTRACT

This study aimed to explore the magnetic resonance cholangiopancreatography (MRCP) manifestations of the pancreaticobiliary ducts and assess pancreatic exocrine function using Secretin-enhanced MRCP (S-MRCP) in dogs with acute edematous pancreatitis (AEP). Twelve (12) dogs were included, with six in the AEP group and six in the control group. The AEP model group underwent a procedure by way of pancreatic duct retrograde injection. The control group underwent the same procedure without infusion. MRCP and S-MRCP were performed identically in both the AEP group and control groups. MRCP was performed pre-surgery and on the 1st, 3rd, and 5th days post-surgery in the AEP group and control groups. The pancreaticobiliary duct diameter was significantly wider in the AEP group compared to the control group (P<0.01) on the 5th day. The S-MRCP images were evaluated on the 3rd day post-surgery at 1, 3, 5, 7, and 11 min after secretin infusion. Compared to the control group, the pancreatic ducts in the AEP group became dilated and branched which appeared, reaching the largest diameters, 3 min postsecretin injection (P<0.01). Eleven minutes after secretin infusion, the degree of duodenal filling in the AEP group was Grade 2, indicating impaired pancreatic exocrine function in dogs with AEP. In conclusion, MRCP provided excellent comprehensive visualization of the pancreatic and hepatobiliary duct systems in dogs with AEP. S-MRCP effectively detected branched pancreatic ducts and impaired pancreatic exocrine in AEP dogs.

To Cite This Article: Yuan Y, Yang DJ, He CO, Shu ZT, Li XK, Yao1 DW, 2024. Evaluation of pancreatic exocrine function by secretin-enhanced magnetic resonance cholangiopancreatography in dogs associated acute edematous pancreatitis. Pak Vet J, 44(3): 721-726. http://dx.doi.org/10.29261/pakvetj/2024.237

INTRODUCTION

Acute edematous pancreatitis (AEP) in dogs is a disease in which pancreatic fluid is overproduced due to various causes, resulting in damage to the pancreatic tissue. Dog of AEP triggers problems such as disruption of pancreatic duct continuity, rupture of the pancreatic ducts, and biliary tract dilatation. Among the many imaging technologies available, ultrasound is widely used for screening pancreatic diseases due to its convenience and affordability (Penninck *et al.*, 2013). However, it has difficulty differentiating and diagnosing pancreatitis, pancreatic abscess, pancreatic neoplasia, and pseudocysts. A study revealed that ultrasound has low sensitivity and specificity in visualizing the pancreatic ducts (Larson, 2016). Computed tomography (CT) was once considered the most effective imaging technique for diagnosing pancreatic diseases (Adrian *et al.*, 2015). However, for some pancreatic diseases, enhancement is required to increase contrast and visualize the necessary imaging features (Ko *et al.*, 2016; Dunn *et al.*, 2024). Moreover, iodine contrast media may aggravate the progression of the disease, and X-ray radiation is unavoidable (Park *et al.*, 2018). CT has poor accuracy in diagnosing pancreatic divisum, and further studies with adjunctive modalities such as magnetic resonance cholangiopancreatography (MRCP) are needed. The lack of radiation exposure, unique soft-tissue contrast, three-dimensional capabilities, and most recently, physiology-based MRI techniques are among the advantages of MRI over CT and ultrasound (Briola, 2022). Endoscopic retrograde cholangiopancreatography (ERCP) is an affordable but technically challenging method for examining pancreatic ducts. Contrast agents are injected into the biliary tract and pancreatic ducts through an endoscope to obtain images of the resulting abnormal dilation, but this is currently difficult to perform clinically in companion animals. MRCP can more accurately reveal the location and extent

of strictures in the biliary tract and pancreatic ducts compared to ERCP (Kumar *et al.*, 2023). MRCP is a widely used, noninvasive imaging technique for visualizing the pancreatic ducts and biliary tract against a background of the original body fluid (Marolf *et al.*, 2013). Based on research findings, MRCP has nearly 90% sensitivity for diagnosing biliary conditions compared with other invasive diagnostic methods like ERCP (Montalvo-Javé *et al.*, 2015). A study found that MRCP with 1.5 Tesla is effective for assessing feline biliary tract and pancreatic ducts when their diameter is >1 mm (Rahmani *et al.*, 2023).

Secretin stimulates the excretion of fluid and sodium bicarbonate from the exocrine pancreas, causing pancreatic duct dilation (Modvig *et al.*, 2020). Secretin-enhanced MRCP (S-MRCP), performed after administering intravenous secretin, provides a dynamic assessment and better visualization of the pancreaticobiliary ductal system than conventional MRCP. S-MRCP may reveal abnormalities that might go undetected on conventional MRCP (Zhang *et al.*, 2013; Briola, 2022). A study suggested the need for secretin while performing MRCP in dogs to optimize the detection of fine biliary and pancreatic ducts (Rahmani *et al.*, 2023). In clinical practice, S-MRCP is a safe, noninvasive technique for simultaneously evaluating morphological and pancreatic exocrine functional characteristics (Swensson *et al.*, 2021).

To date, few MRI studies have been conducted on the imaging characteristics of pancreatic ducts and the biliary tract, and on pancreatic exocrine function in dogs. This study describes the morphological characteristics of the pancreatic ducts and biliary tract, and evaluates exocrine function in dogs with AEP, aiding in clinical diagnosis.

MATERIALS AND METHODS

Animals: The animal study was approved by the institutional animal care and use committee (permit number: NJAU. No20221101315) of Nanjing Agricultural University (Nanjing, China). Twelve adult dogs (half male, half female), 2-4 years old, mixed breed, weighing 10 ± 3.6 kg, were included in this study.

Study design: The dogs were randomly divided into an AEP group (n=6) and a control group (n=6) (Fig. 1).

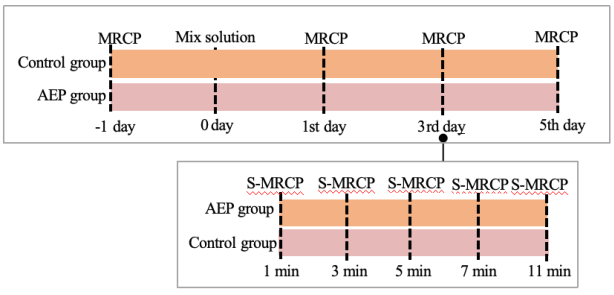

Fig.1: MRCP was performed 1st pre-surgery (-1 day) and on the 1st, 3rd and 5th days post-surgery in both the control group and AEP group. S-MRCP was performed at 1, 3, 5, 7 and 11 min on the 3rd day post-surgery.

Dog AEP model: Retrograde injection was performed to establish a dog model of AEP as previously described (Qin *et al.*, 2007; Van Minnen *et al.*, 2007). The AEP group was injected with a mixture of 5% sodium taurocholate (0.5 mL/kg, McLean Biochemical Technology Co., Ltd., Shanghai, China) and trypsin (3000 U/kg, Baoman Biotechnology Co., Ltd., Shanghai, China). The control group underwent the same surgical procedure without infusion.

Clinical symptoms, hematological and ultrasound examination: clinical signs, physical examination, complete blood count (CBC), serum amylase (Mindray BC-5300 Vet, china), lipase immunoreactivity (Beijing Denotek Technology Co., Ltd.) and ultrasound examination (MyLab™X5, Esaote) were performed in this study.

Histological analysis: On the 5th day post-surgery, the abdominal cavity of a dog in the AEP group and the control group was randomly opened. The pancreatic tissue was immediately, fixed in 4% formaldehyde solution before paraffin wax embedding. After fixed 24 hours, pancreatic tissues were dehydrated, embedded in paraffin, and sectioned into 4 μm thick slices. The sections were then stained with hematoxylin-eosin (H&E) as previously described (Aupperle-Lellbach *et al.*, 2020). The histological characteristics of the pancreas were determined via light microscopy (Ni n ECLIPSE 50i, Japan).

MRCP protocol : MRCP was performed with a 1.5T MRI system (uMR 560 type, Shanghai United Imaging Healthcare Co., Ltd.). The 2D breath-holding T2 weighted single-shot fast spin echo (SSFSE) fat suppression sequence parameters were as follows: TR, 6000 ms; TE, 1000 ms; field of view, 340 × 340 mm; matrix size, 460 × 576; and Slice thickness, 60 mm. The 3D non-breath-holding fat suppression-weighted T2-weighted FSE sequence parameters were as follows: TR, 4000 ms; TE, 650 ms; field of view, 320 × 320 mm; matrix size, 576 × 576; and Slice thickness, 1mm. The diameter of the pancreaticobiliary duct was measured.

S-MRCP examinations: S-MRCP with intravenous injection of secretin at a dose of 50μg/kg (Aladdin, China) was performed identically for the AEP group and control group on the 3th day post-surgery. Pancreatic exocrine function was evaluated by measuring fluid filling in the duodenum via semiquantitative methods and measuring the diameter of the pancreatic ducts. Filling of the duodenum is graded according to duodenal anatomic imaging findings. The grading system was established according to Chamokova *et al.* (2018): Grade 0—no fluid is observed in the duodenum; Grade 1—fluid is limited to the cranial duodenal flexure; Grade 2—fluid partially fills the duodenum up to the caudal duodenal flexure; and Grade 3—fluid fills beyond the caudal duodenal flexure. Pancreatic exocrine function was considered impaired in any animal with Grade <3 (Chamokova *et al.*, 2018).

All animals underwent MRI scanning within 5th post-surgery Animals were treated with intravenous lactated Ringer's solution (100mL/(kg/d), butorphanol (0.6mg/kg IV), and cefazolin (22 mg/kg IV). Animals those vomited were given cerenia (1mg/kg IM, Zoetis, Madison, N., J.,) and intravenously replenished electrolytes and glucose.

Statistical analysis: All images were evaluated on a dedicated workstation (Horos V3.3.1). All values are presented as the means±standard deviation. The data were analyzed by nonparametric statistical tests. The Mann–Whitney U test was used after correcting for intragroup comparisons. All the statistical analyses were performed using GraphPad Prism version 9.0 (San Diego, USA), a value of $P<0.05$ was significant, and a value of significant threshold was set as $P<0.01$.

RESULTS

Clinical symptoms: The clinical symptoms of the AEP group included anorexia, mild vomiting, and abdominal tension. Animals with abdominal pain received butorphanol (0.6mg/kg IV) four times daily for pain management. Lactated Ringer's solution was administered based on the degree of dehydration.

Hematological examination: The white blood cells (WBC), plasma amylase and the plasma lipase levels were significantly increased and peaked in the AEP group on the 1st day post-surgery ($P<0.01$) compared to the control group, indicating pancreatic inflammation (Table 1).

Ultrasound examination: The size of pancreas were significantly increased, and parenchymal echogenicity of the pancreas was heterogeneous on the 1st day post-surgery ($P<0.01$). Cystic echogenic areas were observed in the pancreatic parenchyma on the 1st day post-surgery (Fig. 2B). The pancreas was mildly enlarged, hypoechoic, with peripancreatic hyperechoic mesenteric fat on the 5th day post-surgery (Fig. 2C).

MRCP imaging features of AEP in dogs: Manifestations of pancreatic edema were observed on the 1st and 3rd days (Fig. 4) in the AEP group. Visualization

Table 1: The result of hematological examination.

Detection time	Changes of WBC（×10^9/L）	Plasma levels of amylase (IU/L)	Plasma levels of lipase (ng/mL)
Pre-surgery	10.58 ± 2.87	307.58±28.87	107.58±18.87
1st post-surgery	27.03 ± 5.88**	5900.16±135.88**	1900.16±135.88**
2nd post-surgery	18.56 ± 4.08**	4578.56±127.08**	1578.56±127.08**

Note: *significant difference between the control and AEP group (P<0.05), **significant difference between the control and AEP group (P<0.01).

Table 2: Diameters of the gallbladder (GB), common bile duct (CBD), and hepatobiliary duct (HD) and diameters and classifications of the pancreatic ducts according to MRCP.

Structure	Diameter (mm)	Pre-surgery	Post-surgery 1st day	Post-surgery 3rd day	Post-surgery 5th day
GB	Ctl group	19.49 ± 0.43	18.18 ± 0.39	19.06 ± 0.49	17.85 ± 0.59
	AEP group	18.43 ± 0.57	20.31 ± 0.44	21.57 ± 0.58	29.62 ± 0.73**
CBD	Ctl group	1.81±0.45	1.93±0.24	1.94±0.38	1.87±0.49
	AEP group	1.89±0.39	2.12 ± 0.65	2.15 ± 0.55	3.79 ± 0.68**
HD	Ctl group	1.18±0.23	1.20±0.28	1.19±0.35	1.33±0.31
	AEP group	1.19±0.33	1.24 ± 0.34	1.27 ± 0.39	2.74± 0.47**
PD	Ctl group	Invisible	Invisible	Invisible	Invisible
	AEP group	Invisible	Visible in 1/6 dogs 1.21 ± 0.22	Visible in 4/6 dogs 1.43 ± 0.37	Visible in 6/6 dogs 1.74±0.17**

Note: Ctl: Control. CBD: common bile duct, GB: gallbladder, HD: hepatobiliary duct, RPD: right pancreatic duct, LPD: left pancreatic duct, DP: duodenal papillae. *significant difference between the control and AEP group (P<0.05), **significant difference between the control and AEP group (P<0.01).

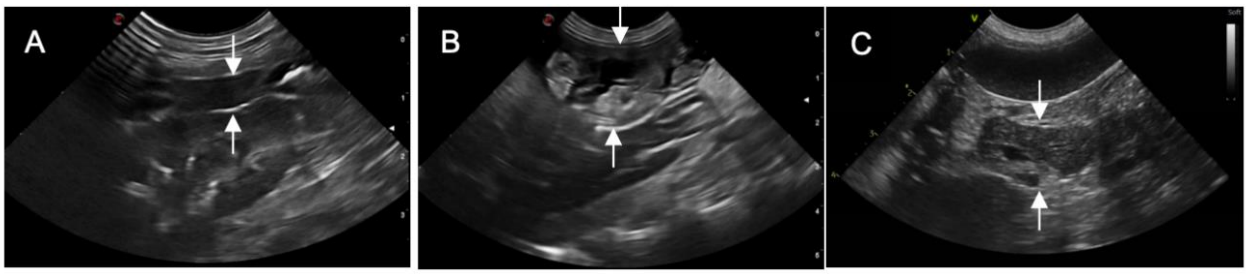

Fig. 2: Ultrasound pancreatic imaging (A) pre-surgery, (B) on the 1st day post-surgery and (C) on the 5th day post-surgery.

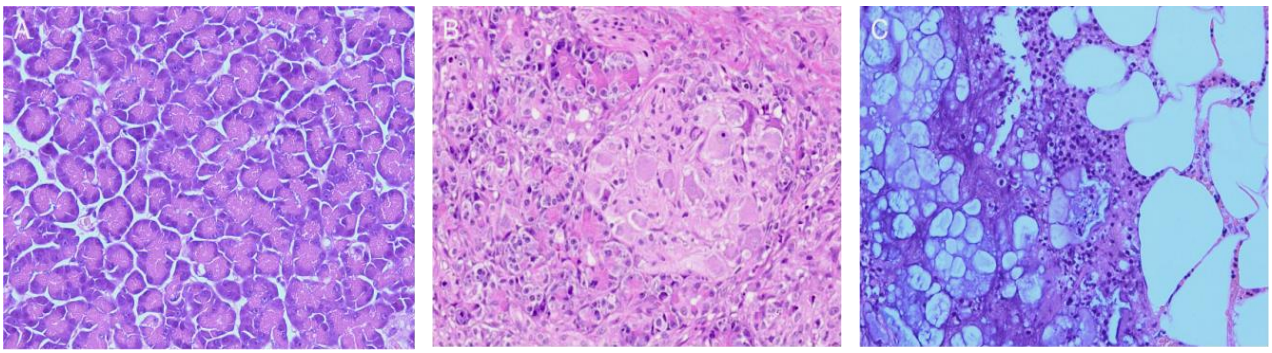

Fig. 3: Histopathological examination of pancreatic tissues. (A) Pancreatic tissue from the control group (200 x), exhibiting normal lobular architecture. (B) Pancreatic tissue from the AEP group (400 x) scale bar = 50 μm), manifestations of interstitial edema. (C) Pancreatic tissue from the AEP group (200 x), showing features of acute pancreatitis.,inflammatory cell infiltration and fat cell necrosis.

MRCP imaging features of AEP in dogs: Manifestations of pancreatic edema were observed on the 1st and 3rd days (Fig. 4) in the AEP group. Visualization for 3/6 dogs in the AEP group on the 5th day revealed that pancreatic ducts were significantly expanded (P<0.01) and demonstrated a "V" shape (Fig. 4). However, the pancreatic ducts were almost invisible in the control group. Both the pancreatic duct and bile duct were dilated in the remaining 3/6 dogs in the AEP group on the 5th day. Compared to the control group, the gallbladder, common bile and hepatobiliary duct were significantly more visible in the AEP group (P<0.01) (Fig. 5).

Pancreatic exocrine function was impaired in AEP dogs according to secretin-enhanced MRCP: Pancreatic ducts were almost invisible in the control group but visible in 4/6 of the dogs in the AEP group before secretin infusion. All dogs in the control group exhibited smoother and more uniform dilation of the pancreatic duct, which reached a maximum diameter at 3 minutes after secretin infusion (Fig. 6). The pancreatic ducts were significantly dilated with discontinuous ducts and branched pancreatic ducts at 1 min after secretin infusion in the AEP group (P<0.05), and this dilation was maintained at 3, 5, 7, and 11 min after secretin infusion (Fig. 7). In the AEP group, the diameter was 1.71±0.31 (P<0.05) compared to the control group (1.21±0.24) at 1 min after secretin infusion. At 3 min, it was 1.30±0.26 in the control group and 2.56 ± 0.36 (P<0.01) in the AEP group. At 5 min, it was 1.15±0.17 in the control group and 2.38±0.43 (P<0.01) in the AEP group. At 7 min, it was 1.13±0.20 in the control group and 2.21±0.39 (P<0.01) in the AEP group. At 11 min, it was 1.07±0.22 in the control group and 1.76±0.24 (P<0.01) in the AEP group.

Before secretin infusion, no obvious liquid signal was observed in the duodenum, and the duodenal filling was classified as Grade 1 in the control group and the AEP group. One minute after secretin infusion, the signal

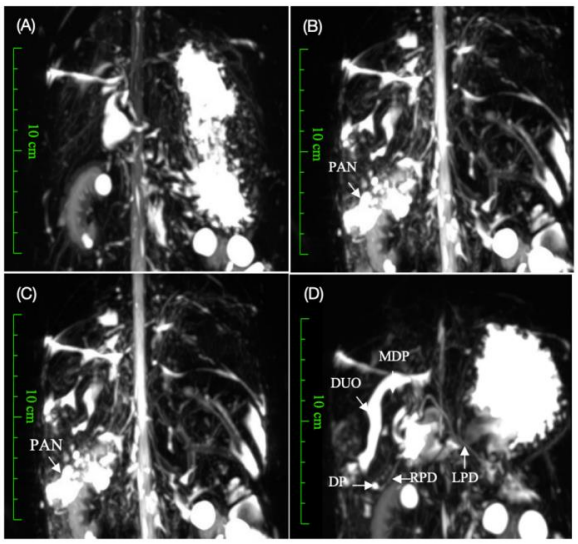

Fig. 4: The pancreatic ducts of dogs in the AEP group gradually widened post-surgery. (A) Pre-surgery. (B) 1st day post-surgery. (C) 3rd day post-surgery. (D) 5th day post-surgery. PAN: pancreas, DUO: duodenum, RPD: right pancreatic duct, LPD: left pancreatic duct, DP: duodenal papilla.

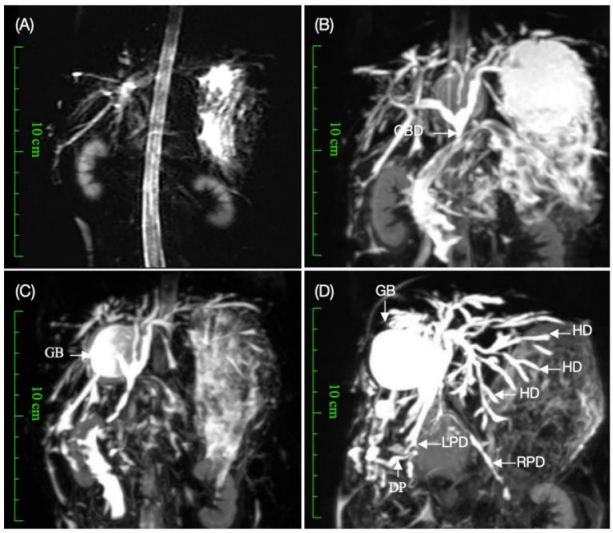

Fig. 5: Both the pancreatic ducts and biliary tract of dogs in the AEP group gradually widened post-surgery. (A) Pre-surgery. (B) 1st day post-surgery. (C) 3rd day post-surgery. (D) 5th day post-surgery. CBD: common bile duct, GB: gallbladder, HD: hepatobiliary duct, RPD: right pancreatic duct, LPD: left pancreatic duct, DP: duodenal papillae.

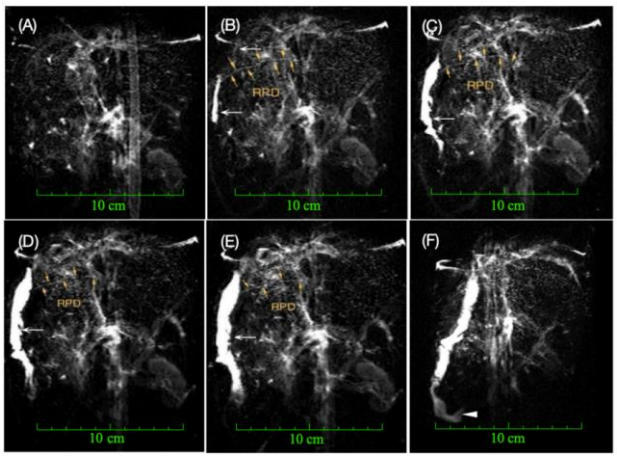

Fig. 6: Features of the pancreatic ducts and duodenal fluid filling in the control group. (A) Image before secretin infusion. (B-F) Images at 1, 3, 5, 7, and 11 min after secretin infusion. The yellow arrow indicates the right pancreatic ducts (RPD) , the white arrow indicates the descending duodenum, and the white arrowhead is the caudal duodenal flexure.

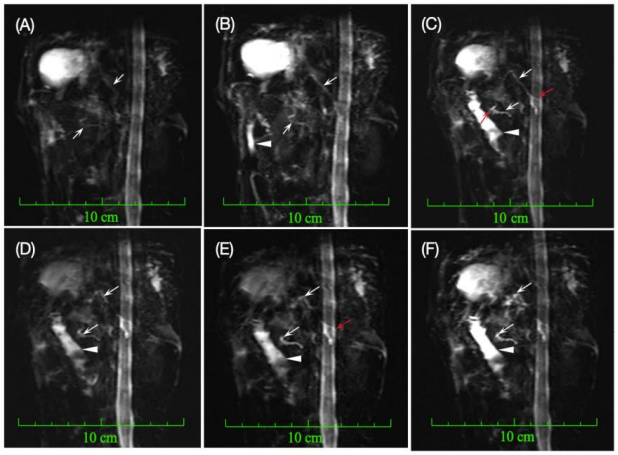

Fig. 7: In the AEP group, fluid filling in the duodenum was reduced, and the pancreatic ducts were less visible. (A) Image before secretin infusion. (B-F) Images at 1, 3, 5, 7, and 11 min after secretin infusion. White arrow, main pancreatic ducts; red arrow, branched pancreatic ducts; white arrowhead, descending duodenum.

intensity representing duodenal filling in was increased, and the filling was classified as Grade 1 in two groups. Three to seven minutes after secretin infusion, the fluid covered the area of the cranial duodenal flexure, reaching the descending duodenum, and the degree of duodenal filling in two groups, and the filling was classified as Grade 1-2 (Fig. 6 and Fig. 7). Eleven minutes after secretin infusion, the duodenum was significantly expanded in the control group, and the liquid reached the caudal duodenal flexure, resulting in a classification of Grade 3 (Fig. 6). However, the AEP group still had Grade 2 at 11 min after secretin infusion suggesting the pancreatic exocrine function of the AEP dogs was impaired (Fig. 7 F).

DISCUSSION

Dogs with AEP showed classic signs of acute pancreatitis, including abdominal tension, vomiting, and anorexia. Blood count, serum amylase, and abdominal ultrasonography may show non-specific findings (Cridge *et al.,* 2021; Kim *et al.,* 2024). However, dog pancreatic lipase immunoreactivity (PLI) has been documented to have a high (90.9%) sensitivity for the diagnosis of acute pancreatitis (Healy *et al.,* 2022). In this study, the result of cPLI was markedly increased, indicating the presence of pancreatitis in the dogs. The specificity of ultrasonography for acute pancreatitis is very high (92%)(Cho *et al.,* 2022). Ultrasonographic findings showed the swollen pancreas with hypoechoic parenchyma indicating inflammatory change and moderately hyperechoic surrounding fats due to fat saponification. Based on Clinical symptoms, hematological examination and ultrasound examination, the diagnosis of acute pancreatitis in the dog was basically confirmed (Rudinsky, 2023; Kim *et al.,* 2024). Moreover, histopathology revealed pancreatic edema, mixed inflammatory cell infiltration, and scattered fat necrosis, which were grossly apparent in the AEP group but absent in the control group. According to clinical presentation, dog acute pancreatitis can vary from mild to moderate clinical signs (AEP) to severe, life-threatening disease caused by acute necrotizing pancreatitis (ANP)(Vrolyk and Singh, 2020; Bjørnkjær-Nielsen and Bjørnvad, 2021). Early diagnosis of AEP can help prevent progression to ANP.

Previous research on feline pancreatitis suggested that MRCP is an advantageous supplemental sonography method for visualizing the pancreatic ducts in cats (Marolf *et al.,* 2011). This study indicated that MRCP images provided an comprehensive view of the pancreatic and hepatobiliary ducts without shading by the bowel, which can occur on ultrasound. However, in contrast to other studies, our pilot study was conducted to visualize the pancreatic ducts of AEP dogs. A postmortem study showed the visualizition of the pancreaticobiliary duct in dogs, which showed feasibility of MRCP in live dogs (Rahmani *et al.,* 2024). In a postmortem study, involving 5 out of 8 mixed-breed dogs, the average age was 13.5 years, and the average weight was 15.3kg. However, pancreatic duct structures smaller than 1mm were difficult to visualize using a 1.5 Tesla MRI magnet (Rahmani *et al.,* 2023). Pancreatitis resulting in hepatic biliary obstruction can cause substantial morbidity and mortality. In this study, three of the dogs with AEP showed severe dilatation of pancreaticobiliary duct on the 5th day post-surgery. Three of the dogs with AEP had severe pancreatic duct distention beginning on the 5th day post-surgery. The dilatation of pancreaticobiliary ducts was likely secondary to ductal obstruction caused by edema in the pancreas, duodenum, or duodenal papilla. The risk of general anesthesia and associated costs limit the use of MRCP in animals. However, some of the advantages of MRCP may justify this approach, particularly in situations where ultrasound results are equivocal. An ultrasonographic study of 242 dogs (body weight 1.4-55kg) revealed that the diameters of the pancreatic ducts ranged between 0.4 and 1.2 mm and were significantly correlated with body weight (Penninck *et al.,* 2013). Regarding limitations, this study did not include larger or smaller dogs, different breeds, or younger and older dogs. These limitations negatively impacted the results of the study. Further studies are warranted to adapt magnetic resonance cholangiopancreatography to the diagnostic needs of those dogs. In this study, S-MRCP was optimal for visualizing tiny structures such as pancreatic ducts in small dogs.

Evaluation of pancreatic duct dynamics is possible only with MRCP images obtained before and after S-MRCP (Briola, 2022). Healthy pancreatic parenchyma and pancreatic ducts have suitable elasticity to facilitate the outflow of pancreatic juice without causing dilatation of the pancreatic ducts. In this study, the mean diameter of the pancreatic ducts was less than 1.5mm at different post-surgery time points after secretin injection in the control group, and branched pancreatic ducts were not visible. However, the mean diameter of the pancreatic ducts was greater than 2.5mm at different post-surgery time points in the AEP group, and branched pancreatic ducts were also visible. This study found that branched pancreatic ducts were visible, and pancreatic fluid leakage was confirmed in the AEP group. According to a study of exocrine pancreatic insufficiency in clinical dogs and cats, the abnormal exocrine function of the pancreas is commonly caused by pancreatic duct obstruction (Kennedy and Williams, 2012). In this study, S-MRCP revealed discontinuity of the pancreatic ducts with varying diameters in AEP dogs. Unlike the control group, the AEP group presented with obstructions in the pancreatic ducts, which indicated abnormal pancreatic exocrine function. Pancreatic exocrine function was evaluated using semiquantitative or quantitative methods after S-MRCP. In this study, S-MRCP showed the degree of duodenal filling and the leakage of the pancreatic duct simultaneously, which is more practical for veterinary clinical practice. Regarding limitations, the S-MRCP study did not include quantitative methods (Zhang *et al.,* 2013). Further studies are warranted to apply S-MRCP with the aim of quantifying pancreatic exocrine function in AEP dogs.

Conclusions: The results indicate that MRCP provided excellent comprehensive visualization of pancreatic duct and hepatobiliary duct systems and pancreatic edema lesions in AEP dogs. When ultrasound results are equivocal or the pancreas is incompletely assessed

sonographically owing to bowel gas or lack of compliance, MRCP becomes particularly valuable. Furthermore, MRCP for diseases related to canine pancreatic and bile ducts showed important clinical significance. MRCP examination should be considered a potentially valuable diagnostic method. The study showed that the pancreatic ducts of normal dogs were almost invisible through MRCP, demonstrating that S-MRCP is a feasible way to visualize the pancreatic ducts in dogs S-MRCP was a feasible alternative to other techniques for assessing pancreatic exocrine function in dogs with AEP.

Acknowledgements: This study was supported by the Ruipeng Foundation and New Ruipeng Pet Healthcare Group (RPJJ2020018) and the Fundamental Research Funds for the Central Universities (KYYJ202104).

Authors contributions: Yue Yuan, De Ji Yang，Da Wei Yao and Xiao Kun Li conceived and designed the study. Chu Qiao He and Zong Tao Shu executed the experiment and analyzed the sera and tissue samples. Yue Yuan analyzed the data.

REFERENCES

Adrian AM, Twedt DC, Kraft SL, *et al.*, 2015. Computed Tomographic Angiography under sedation in the diagnosis of suspected canine pancreatitis: A pilot study. J Vet Intern Med 29:97-103.

Aupperle-Lellbach H, Törner K, Staudacher M, *et al.*, 2020. Histopathological findings and canine pancreatic lipase immunoreactivity in normal dogs and dogs with inflammatory and neoplastic diseases of the pancreas. J Vet Intern Med 34:1127-1134.

Bjørnkjær-Nielsen KA and Bjørnvad CR, 2021. Corticosteroid treatment for acute/acute-on-chronic experimental and naturally occurring pancreatitis in several species: a scoping review to inform possible use in dogs. Acta Vet Scand 63: 28.

Briola C, 2022. Magnetic resonance imaging and magnetic resonance imaging cholangiopancreatography of the pancreas in small animals. Vet Sci 9: 378.

Chamokova B, Bastati N, Poetter-Lang S, *et al.*, 2018. The clinical value of secretin-enhanced MrcP in the functional and morphological assessment of pancreatic diseases. Br J Radiol 91: 20170677. doi: 10.1259/bjr.20170677

Cho H, Yang S, Suh G, *et al.*, 2022. Correlating two-dimensional shear wave elastography of acute pancreatitis with Spec cPL in dogs. J Vet Sci 23:1-11.

Cridge H, Twedt DC, Marolf AJ, *et al.*, 2021. Advances in the diagnosis of acute pancreatitis in dogs. J Vet Intern Med 35:2572–2587.

Dunn A, Rao S, Husbands B, *et al.*, 2024. Computed tomographic features of exocrine pancreatic carcinomas in dogs and cats. Veterinary Radiology and Ultrasound 65:400–407.

Healy DM, Cassidy JP and Martin SA, 2022. A true congenital pancreatic cyst in a dog. BMC Vet Res 18:1–7.

Kennedy OC and Williams DA, 2012. Exocrine pancreatic insufficiency in dogs and cats: Online support for veterinarians and owners. Top Companion Anim Med 27:117–122.

Kim JK, Hwang SY, Kim SE, *et al.*, 2024. A comparative analysis of canine pancreatic lipase tests for diagnosing pancreatitis in dogs. J Vet Sci 25:1–12.

Kim K, Kim H, Joo JB, *et al.*, 2024. Evaluation of the clinical usefulness of pancreatic alpha amylase as a novel biomarker in dogs with acute pancreatitis: a pilot study. Vet Q 44:1–7.

Ko SE, Choi IY, Cha SH, *et al.*, 2016. Clinical and radiologic characteristics of pancreatic head carcinoma without main pancreatic duct dilatation: Using dual-phase contrast-enhanced CT scan. Clin Imaging 40:548–552.

Kumar A, Mohanty NR, Mohanty M, *et al.*, 2023. Comparison of MRCP and ERCP in the evaluation of common bile duct and pancreatic duct pathologies. Front Med Technol 5:1–7.

Larson MM, 2016. Ultrasound Imaging of the Hepatobiliary System and Pancreas. Vet Clin North Am Small Anim Pract 46:453–480.

Marolf AJ, Kraft SL, Dunphy TR, *et al.*, 2013. Magnetic resonance (MR) imaging and MR cholangiopancreatography findings in cats with cholangitis and pancreatitis. J Feline Med Surg 15:285–294.

Marolf AJ, Stewart JA, Dunphy TR, *et al.*, 2011. Hepatic and pancreaticobiliary mri and mr cholangiopancreatography with and without secretin stimulation in normal cats. Vet Radiol Ultrasound 52:415–421.

Modvig IM, Andersen DB, Grunddal K V, *et al.*, 2020. Secretin release after Roux-en-Y gastric bypass reveals a population of glucose-sensitive S cells in distal small intestine. Int J Obes 44:1859–1871.

Montalvo-Javé EE, Mendoza Barrera GE, Valderrama Treviño AI, *et al.*, 2015. Absorbable bioprosthesis for the treatment of bile duct injury in an experimental model. Int J Surg 20:163–169.

Park HY, Cho YG, Lee YW, *et al.*, 2018. Evaluation of gallbladder and common bile duct size and appearance by computed tomography in dogs. J Vet Sci 19:653–659.

Penninck DG, Zeyen U, Taeymans ON, *et al.*, 2013. Ultrasonographic measurement of the pancreas and Pancreatic Duct in Clinically Normal Dogs. Am J Vet Res 74: 433–437.

Qin HL, Su ZD, Hu LG, *et al.*, 2007. Effect of parenteral and early intrajejunal nutrition on pancreatic digestive enzyme synthesis, storage and discharge in dog models of acute pancreatitis. World J Gastroenterol 13:1123–1128.

Rahmani V, Peltonen J, Amarilla SP, *et al.*, 2023. Cholangiopancreatography in cats: a post-mortem comparison of MRI with fluoroscopy, corrosion casting and histopathology. Vet Radiol Ultrasound 64:713–723.

Rahmani V, Peltonen J, Amarilla SP, *et al.*, 2023. Feasibility of Magnetic Resonance Cholangiopancreatography in Dogs—A Post-Mortem Study. Animals 13: 2517

Rahmani V, Peltonen J, Hmelnikov D, *et al.*, 2024. Three-dimensional magnetic resonance cholangiography is superior to two-dimensional single-shot magnetic resonance cholangiography for visualization and image quality of the feline and canine biliary tract: A postmortem study. Vet Radiol Ultrasound 65:377–384.

Rudinsky AJ, 2023. Laboratory Diagnosis of Pancreatitis. Vet Clin North Am Small Anim Pract 53:225–240.

Swensson J, Zaheer A, Conwell D, *et al.*, 2021. Secretin-enhanced MRCP: How and Why-AJR expert panel narrative review. AJR Am J Roentgeno 216:1139–1149.

Van Minnen LP, Blom M, Timmerman HM, *et al.*, 2007. The use of animal models to study bacterial translocation during acute pancreatitis. J Gastrointest Surg 11:682–689.

Vrolyk V and Singh B, 2020. Animal models to study the role of pulmonary intravascular macrophages in spontaneous and induced acute pancreatitis. Cell Tissue Res 380:207–222.

Zhang TT, Wang L, Wang D Bin, *et al.*, 2013. Correlation between secretin-enhanced MRCP findings and histopathologic severity of chronic pancreatitis in a cat model. Pancreatology 13:491–497.